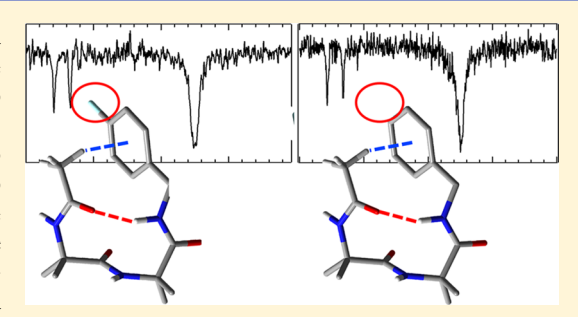
Single-Conformation Spectroscopy of Capped Aminoisobutyric Acid Dipeptides: The Effect of C-Terminal Cap Chromophores on Conformation

Joshua L. Fischer,[†] Brayan R. Elvir,[‡] Sally-Ann DeLucia,[‡] Karl N. Blodgett,[†] Matthias Zeller,[†] Matthew A. Kubasik,[‡] and Timothy S. Zwier*,[†]

Supporting Information

ABSTRACT: Aminoisobutyric acid (Aib) oligomers are known to form racemic mixtures of enantiomeric left- and right-handed structures. The introduction of a chiral cap converts the enantiomeric structures into diastereomers that, in principle, afford spectroscopic differentiation. Here, we screen different C-terminal caps based on a model Aib dipeptide using double resonance laser spectroscopy in the gas phase to record IR and UV spectra of individual conformations present in the supersonic expansion: NH-benzyl (NHBn) as a reference structure because of its common use as a fluorophore in similar studies, NH-pfluorobenzyl (NHBn-F), and α -methylbenzylamine (AMBA). For both the NHBn and NHBn-F caps, a single conformer is observed, with



infrared spectra assignable to an enantiomeric pair of type II/II' β -turns in these molecules lacking a chiral center. The higher oscillator strength of the NHBn-F cap enabled UV-UV hole burning, not readily accomplished with the NHBn cap. The AMBA-capped structure, with its chiral center, produced two unique conformers, one of which was a nearly identical lefthanded type II β -turn, while the minor conformer is assigned to a C7-C7 sequential double ring, which is an emergent form of a 2_7 -ribbon. Although not observed, the type II' β -turn diastereomer, with opposite handedness, is calculated to be 11 kJ/mol higher in energy, a surprisingly large difference. This destabilization is attributed primarily to steric interference between the Cterminal acyl oxygen of the peptide and the chirality-inducing methyl of the AMBA group. Last, computational evidence indicates that the use of an N-terminal aromatic cap hinders the formation of a 3₁₀-helix in Ac-Aib₂ dipeptides.

1. INTRODUCTION

The forces giving rise to well-structured peptides and proteins have been of interest for decades. 1-3 In the 1950s, Pauling and co-workers emphasized hydrogen bonding interactions in discerning α helices and β sheets, the two dominant secondary structural motifs of proteins.⁴ Donohue soon followed Pauling's α helix by proposing the 3_{10} helix.⁵ These two helical forms, the α helix and the 3_{10} helix, are regularly observed in protein structures and are supported by intrabackbone hydrogen bonds that close 13- and 10-membered rings (C13 and C10), respectively, requiring only slight variations in ϕ/ψ backbone angles. Additional C10 structures, β -turns requiring only four successive residues, were first reported by Venkatachalum. While the repeating backbone ϕ ψ angles of the 3₁₀-helix $(-60^{\circ}/-30^{\circ})$ comprise type III turns, type I and type II C10 structures require nonrepeating ϕ/ψ angles along the peptide backbone chain to "turn" its direction.6

Despite early emphasis on hydrogen bonding patterns, the modest stability of folded proteins, relative to their unfolded configurations, means that a variety of forces, including shortrange van der Waals forces, as well as hydrogen bonding, are important for the unique folds of proteins. 1,2 For example, single methylation and double methylation of glycine's α carbon (e.g., Gly vs Ala vs Aib) provide a dramatic increase in the residue's helicogenicity.

In biological settings, most proteinogenic helices are righthanded α -helices having 3.6 residues/turn, with $\phi/\psi = -60^{\circ}$ / -45°, supported by NH···O=C hydrogen bonds that close 13-membered rings (referred to as C13 hydrogen bonds).^{8,9} The 3₁₀-helix comprises about 10% of protein helices and is wound more tightly, with 3.0 residues/turn, $\phi/\psi \cong -57^{\circ}/-$ 30°, forming a series of C10 hydrogen bonds. 5,9 Interestingly, in room-temperature solution, the ϕ/ψ angles for a 3₁₀-helix are rather loosely defined because of the steric strain resulting from the necessary residue overlap of a helix having an integer number of residues/turn. In some cases, α - and 3_{10} -helices can interconvert, and it has been suggested that the 3₁₀-helix could be an intermediate state for the formation of α -helices. ^{10,11} Indeed, the balance between α -helix and 3_{10} -helix

Received: February 21, 2019 Revised: April 11, 2019 Published: April 11, 2019

[†]Department of Chemistry, Purdue University, West Lafayette, Indiana 47907, United States

[‡]Department of Chemistry and Biochemistry, Fairfield University, Fairfield, Connecticut 06824, United States

can be tipped by the presence of even one amino acid that directs formation of one helix over the other, ^{12,13} suggesting that the C10 versus C13 hydrogen bonding pattern is not by itself determinative.

Aminoisobutyric acid (Aib) is a nonproteinogenic, naturally occurring amino acid with geminal methyl groups substituted on the α -carbon, which is known to favor 3_{10} -helix formation. 14,15 The symmetric methyl substitution renders Aib achiral, removing the chiral influence directing helix formation and rendering left- and right-handed helices of poly-Aib peptide enantiomers equivalent in energy. Aib is most commonly found naturally in the peptaibol family of antimicrobial peptides, 15,16 which have been used in foldamer studies to generate transmembrane pores.¹⁷ The heliogenic character imparted by Aib is believed to drive the formation of these transmembrane pores, which result in antimicrobial activity. 17 Vibrational modes of the polar amide groups inherent to peptides are highly sensitive to their local environment, including their hydrogen bonding network, and consequently are diagnostic of the secondary structures adopted by peptides and proteins. The NH stretch frequencies found in the amide A region shift to lower frequencies with increasing hydrogen bond strength, providing a particularly useful diagnostic. However, in aqueous solution, these absorptions occur in the midst of the broad OH stretch band, masking their presence. Using nonpolar CDCl3 to minimize spectral interference, Toniolo and co-workers have studied a set of Z-(Aib), OtBu (n = 1-12) peptides in the amide A region that pointed to these peptides undergoing 310helix formation in nonpolar solvents. 14 These authors identified two NH stretch fundamentals assigned to "free" and "intramolecularly hydrogen-bound" NH groups. As n increases, the "hydrogen-bound" band grew at the expense of the free NH stretch band. Decades later, Maekawa et al. used two-dimensional IR spectroscopy in the amide I region (n = 3, 5, 8, 10) to investigate the C=O stretch vibrations and showed that the onset of 3_{10} -helix formation occurs with n >5. More recently, infrared spectra from some of us, using 13Cisotopologues of Z-(Aib)₆-OtBu, showed isotope-shifted localized ¹³C=O amide I modes that confirmed 3₁₀-helix formation.¹⁹ Although isotope editing singles out the local mode absorptions of individual ¹³C=O subunits by shifting their absorptions to lower frequencies, these spectra are still influenced by solvent effects.

Studying the intramolecular interactions of peptides under jet-cooled conditions in the gas phase provides the unique opportunity to interrogate the peptides without solvent influence. Often, gas-phase studies of peptides are difficult because peptides are nonvolatile, necessitating laser desorption to bring them into the gas phase. Furthermore, most do not have a natural chromophore to sensitize their detection. Previous work has used phenyl ring caps as chromophores at either terminus of the peptides. 25-33 However, weak chromophore absorption, low number densities, and shot-toshot fluctuations associated with laser desorption indicate that further experimental improvements would be welcome. Even with these shortcomings, desorption experiments have been used successfully to interrogate a range of peptides in the gas phase.²²⁻⁴⁰ The hydrogen-bonded networks present in these peptides can be probed in exquisite detail through the NH stretch and amide I/II regions, which reflect the hydrogenbonded network present in the peptide. Comparisons of highquality quantum chemical calculations routinely confirm the spectral assignments.

The present study on capped Aib peptides has as one point of comparison an earlier study from our group on the gasphase conformational preferences of Z-capped oligo-glycines up to n=5. Because glycine is the only naturally occurring achiral amino acid, with its two hydrogen atoms on $C(\alpha)$, it is a seemingly close analogue of the Aib peptides studied here. Interestingly, Z-(Gly)₅ folds not into an α - or 3₁₀-helix but instead into an emergent form of a 14-/16-mixed helix, with amide—amide hydrogen bonds in alternate directions, $N \rightarrow C$ and $C \rightarrow N$.

Mons and co-workers have studied the single-conformation spectroscopy of a capped tripeptide, Ac-Aib-Phe-Aib-NH₂, under jet-cooled conditions.²⁴ In that case, the amide NH stretch spectrum of the main conformer was assigned to a structure containing two C10 hydrogen bonds, indicating incipient 3₁₀-helix formation, with C10 NH stretch fundamentals at 3374 and 3405 cm⁻¹. Expanding upon this work, Gord and co-workers studied a series of Aib-oligomers with benzoylcarboxy (Z) and methyl ester (OMe) caps at the Nand C-termini, respectively: (Z)-Aib_n-OMe (n = 1, 2, 4).³¹ The smaller n = 1,2 peptides formed conformers that exhibited Ramachandran angles similar to those in a 3_{10} -helix, while the n= 4 peptide had sufficient length to fold into an incipient 3_{10} helix, identified by two characteristic C10 hydrogen bonds with NH stretch fundamentals at 3383 and 3406 cm⁻¹ and two free NH stretch transitions.

In the current work, we study three short peptides of the form Ac-Aib-Aib-R, where the C-terminus is a benzyl amide or a substituted benzyl amide. These molecules are capable of forming C10 structures, including a single type III β -turn, which has the same Ramachandran angles as those present in 3₁₀-helix formation. We employ single-conformation gas-phase spectroscopic techniques, coupled with quantum chemical computations, to determine gas-phase conformations of these three molecules, with R being a benzylamide, a para-fluorobenzylamide, and a chiral (S)- α -methyl benzyl amide. These molecules are part of a longer-term research project to study peptides capable of forming both left- and right-handed helices. Although these structures themselves are too small to produce fully formed 3₁₀-helices, their elongated versions of the benzyl amide and the fluorobenzyl amide would have left- and righthanded 3₁₀-helices that are equal in energy. By adding a chiral α -methyl (S) chromophore cap, we introduce a slight steric asymmetry in order to probe its effect on the structure adopted by the parent peptides and probe the right- and left-handed structures that emerge. Last, we test the fluorinated phenyl ring as the chromophore cap to see the effects of its stronger absorption on signal size and whether fluorination changes the conformational preferences.

2. METHODS

2.1. Experimental Section. Solid sample was brought into the gas phase using laser desorption by crushing the sample into a fine powder, mixing the powder into the surface of a flat graphite bar, and then desorbing the sample into the gas phase using the 1064 nm fundamental of a Nd:YAG laser operating at 20 Hz (Continuum Minilite II, ~4 mJ/pulse, 2 mm beam diameter). The resulting desorption plume was entrained orthogonally into the high-collision regime of a supersonic expansion to cool conformers to their zero-point vibrational levels. The expansion was generated with a pulsed valve

(Parker, Series 9, 1 mm dia. nozzle, 4 bar backing pressure Ar, 20 Hz, 500 μ s pulse duration). The resulting free jet was skimmed through a 3 mm conical skimmer ~2-3 cm downstream from the pulsed valve orifice, forming a molecular beam that entered the extraction region of a Wiley-McLaren time-of-flight mass spectrometer, where single and double resonance laser spectroscopy techniques were used to interrogate the sample.

Figure 1 illustrates the set of laser-based methods used in this study. The UV spectrum of the three molecules in the

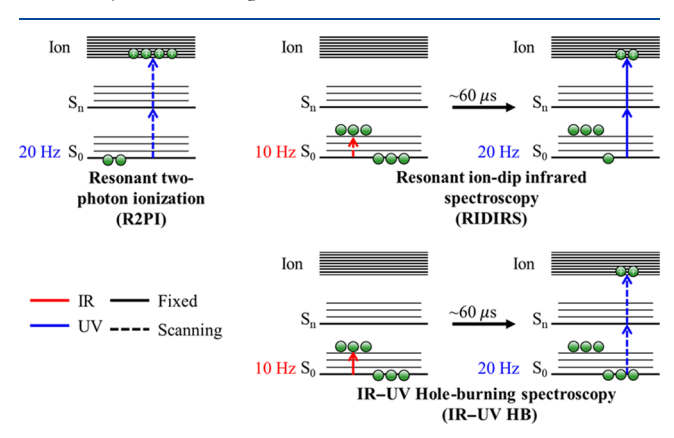


Figure 1. Schematic for double resonance techniques using a 60 μ s delay between the first and second lasers.

series was recorded in the S_0-S_1 origin region using one-color, resonant two-photon ionization (R2PI). Ions were generated by introducing the frequency doubled output of a tunable dye laser into the ion source region of the time-of-flight mass spectrometer. A Radiant Dyes Narrowscan dye laser (Coumarin 540A) pumped with the third harmonic from a Nd:YAG laser (Continuum, Surelite II) was used for this purpose. The R2PI spectrum in the UV region is recorded by monitoring the ion intensity in the parent mass channel as a function of the UV frequency in the region of the S_0-S_1 origin for each unique aromatic cap (R = NHBn or AMBA, 37 400- $37\,800 \text{ cm}^{-1}$; R = NHBn-F, $36\,900-37\,200 \text{ cm}^{-1}$). By cooling the conformers to their zero-point vibrational levels, there is no contribution to the spectrum from vibrational hot bands, reducing spectral complexity to the point that electronic transitions for specific conformers can be resolved.

Double resonance techniques were used to record singleconformation IR and UV spectra. These methods depend on depleting the population of a single conformer in its zero-point vibrational level, being monitored via R2PI. In resonant-ion dip infrared spectroscopy (RIDIRS), the UV laser (20 Hz) has its wavelength fixed on a conformer-specific UV transition, generating a 20 Hz ion signal in the parent mass channel. The IR laser (10 Hz) was aligned antiparallel to the molecular beam and set to temporally precede the UV laser such that the laser pulse intersects the molecular beam as it passes through the skimmer cone, ~60 µs before the UV laser. This configuration ensures that the maximum number of skimmed, jet-cooled molecules are exposed to the IR laser. The IR laser is scanned in wavelength, and when the IR laser is resonant with a vibrational transition of the same conformation being monitored by the UV laser, population is removed from the zero-point vibrational level to an excited vibrational state, leading to depletion in the R2PI signal of the monitored zeropoint level. The repetition rates of the lasers create an

alternating IR-on/IR-off scheme. The difference signal from successive UV laser pulses (one with IR, one without) is recorded using a gated integrator (Stanford Research Systems, SR 250) in active baseline subtraction mode, which outputs the difference of IR-off and IR-on ion signals as a function of the tuned frequency of the IR laser.

To produce conformer-specific UV spectra via IR-UV holeburn (IR-UV HB) spectroscopy, the same laser scheme as RIDIRS is used, except the wavelength of the IR laser is fixed on a conformer-specific IR transition, while the UV laser is tuned across a frequency range. As in RIDIRS, the IR-UV HB spectra were generated by plotting the difference of the IR-off and IR-on ion signals as a function of UV frequency. In the fluorinated, NHBn-F-capped molecule, the larger oscillator strength of the electronic transition made it possible to record a conformer-specific UV spectrum using UV-UV hole burning. In this case, a UV hole-burn laser is fixed on a UV transition, partially depleting its ground-state zero-point level population.

Conformation-specific IR spectra were acquired using a Nd:YAG-pumped KTP/KTA optical parametric converter (LaserVision), generating light in the amide A (NH stretch) region (3200-3500 cm⁻¹, 20-25 mJ/pulse). Light for the amide I/II regions was generated by difference frequency mixing the output from the optical parametric converter in a AgGaSe₂ crystal (1400–1800 cm⁻¹, 0.75–1.50 mJ/pulse), which was then focused using a 500 mm CaF₂ lens.

Synthesis of the molecules was carried out at Fairfield University. The most direct synthesis of the three peptide samples was to couple the oxazolone of Ac-Aib-Aib-OH to the three different amine caps in dry MeCN (overnight reflux). 41,42 After isolation, the peptides were purified using flash silica gel chromatography. Crystals for X-ray analysis were grown via diffusion of diethyl ether into a solution of methylene chloride.

2.2. Computational Studies. A conformational search of the potential energy surface was performed using the Amber* force field in the Macromodel software suite. 43 The 100 lowest energy structures within 50 kJ/mol of the global minimum were submitted to geometry optimization (tight optimization) and frequency calculations using density functional theory calculations that employed the B3LYP functional with a Grimme dispersion correction [density functional theory (DFT) B3LYP-D3BJ] with a 6-31+G(d) basis set, using the Gaussian 09 software package. 44 Tight optimization conditions were employed. Harmonic vibrational frequencies were calculated at the same level of theory and were scaled to account for anharmonicity using the accepted values of 0.958 for the NH stretch region, 0.981 for the amide I region, and 0.970 for the amide II region.^{28-31,45}

2.3. Crystallography Studies. A single crystal of AMBA-F was coated with Fomblin oil and transferred to the goniometer head of a Bruker Quest diffractometer with kappa geometry, an I-μ-S microsource X-ray tube, laterally graded multilayer (Goebel) mirror single crystal for monochromatization, a Photon2 CMOS area detector, and an Oxford Cryosystems low-temperature device. Examination and data collection were performed with Cu K α radiation ($\lambda = 1.54178$ Å) at 150 K. Data were collected, reflections were indexed and processed, and the files were scaled and corrected for absorption using APEX3.46 The space group was assigned, and the structures were solved by direct methods using XPREP within the SHELXTL suite of programs⁴⁷ and refined by full matrix least squares against F^2 with all reflections with Shelxl2018 using the graphical interface Shelxle. H atoms attached to carbon atoms were positioned geometrically and constrained to ride on their parent atoms. C-H bond distances were constrained to 0.95 Å for aromatic C-H moieties and to 1.00 and 0.98 Å for aliphatic C-H and CH₃ moieties, respectively. Water and amide H atom positions were refined, and O-H and N-H distances were restrained to 0.84(2) and 0.88(2) Å, respectively. $U_{iso}(H)$ values were set to a multiple of $U_{eq}(C)$ with 1.5 for CH₃ and OH and 1.2 for C-H and N-H units, respectively. The water molecule site was found to be partially occupied. The occupancy was refined to 94.0(7)%. Additional data collection and refinement details in table format can be found in the Supporting Information. Complete crystallographic data, in CIF format, have been deposited with the Cambridge Crystallographic Data Centre. CCDC 1898412 contains the supplementary crystallographic data for this paper. These data can be obtained free of charge from The Cambridge Crystallographic Data Centre via www.ccdc.cam. ac.uk/data_request/cif.

3. RESULTS

Three peptide caps were chosen for this study, shown in Figure 2. In what follows, the "R" labels in the figure will serve as

Figure 2. (a) Diagram depicting the Ramachandran ϕ/ψ angles of a peptide, which determine the secondary structure according to the Ramachandran plot. (b) Aib backbone structure with the three R caps used in this study. The shorthand used throughout the text is the text beneath the respective R group.

shorthand designations for each Ac-Aib2-R molecule. The Aib dipeptide with an NHBn cap serves as a reference, as our group most commonly studies peptides with this cap, ²⁹⁻³³ The NHBn-F cap is designed to increase the oscillator strength of the $S_0 \rightarrow S_1$ transition, the region where we carry out our UV spectroscopy. This cap may also weaken $NH \cdots \pi$ interactions by withdrawing electron density from the π cloud on the phenyl ring. Last, the AMBA cap will be used to introduce a chiral center outside of the folding region of the peptide, converting any left- or right-handed enantiomeric secondary structures found in NHBn into diastereomers that can be spectroscopically distinguished.

3.1. Nomenclature. We label an intramolecular hydrogen bond using the symbol "Cn", where n denotes the size of the ring the hydrogen bond closes. For example, a structure that has a NH···O=C hydrogen bond that closes off a 10membered ring is labeled as a C10 hydrogen bond. As a shorthand method for naming the capped dipeptide structures, we adopt a nomenclature used in previous work:³¹ Starting from the N-terminus and proceeding to the C-terminus, each successive amide NH group in the structure is characterized by

the type of hydrogen bond in which this NH group is involved. A free NH is denoted by "F", a Cn hydrogen bond by "n", or an NH··· π -interaction by " π ". For example, the assigned β -turn for NHBn contains two free NH bonds: NH(1) and NH(2), with NH(3) engaging in a C10 hydrogen bond, thereby labeled as F-F-10. Throughout this work, right- and left-handed turns are chiral secondary structural elements that are at times referred to as enantiomers of one another; similarly, the presence of a single chiral center in conjunction with a chiral structural element is referred to as a diastereomer. The left-/right-handed forms of the β -turns are designated as II/II', III/III', and so

3.2. Ac-(Aib)₂-NHBn. The R2PI (black, top) and IR-UV HB (red, bottom) spectra are shown in Figure 3. Most of the

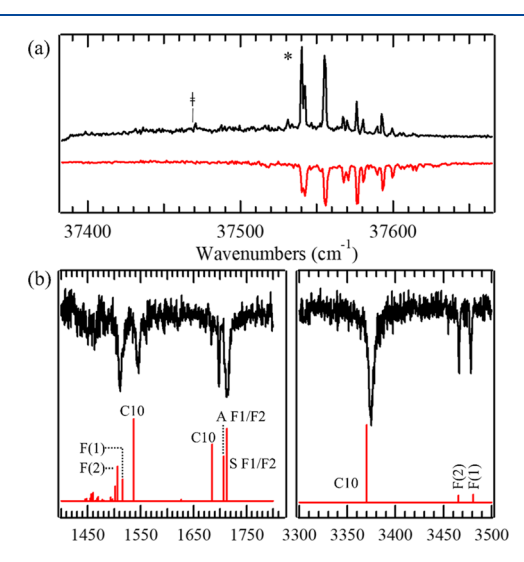


Figure 3. (a) R2PI and IR-UV HB spectra of Ac-(Aib)₂-NHBn. (b) RIDIR spectra for Ac-(Aib)₂-NHBn. The experimental vibrational spectra on top (black) cover the amide II region (1400–1600 cm⁻¹), the amide I region (1600-1800 cm⁻¹), and the NH stretch region (3300-3500 cm⁻¹). The predictions of DFT B3LYP/D3BJ 6-31+G*(d) calculations are shown in red below.

transitions found in the R2PI spectrum are reproduced in the IR-UV HB spectra, indicating that there is one major conformer, with its S_0-S_1 origin transition at 37 540 cm⁻¹. Close inspection of the region near 37 470 cm⁻¹ shows a small transition, marked with a dagger, which is part of a broad background not present in the IR-UV HB spectra. This transition may belong to a low population second conformer; however, there was not enough signal to perform double resonance experiments on it. In addition, there is a 2 cm⁻¹ splitting of the origin. However, we verified that both peaks involved in the splitting belong to the same conformer: RIDIR spectra taken on both peaks produced identical IR spectra. Additionally, because of the consistent difference in relative intensities of the doublet between the IR-UV HB and R2PI spectra, IR-UV HB spectra were taken using all the peaks in the NH stretch region and one peak in the amide I region (1697 cm⁻¹) as hole-burn transitions, with all scans modulating the intensities of the same set of UV transitions, as shown in Figure 3. This shoulder is then most likely a sequence band from the same conformer.

The RIDIR spectrum of this main conformer of Ac-(Aib)₂-NHBn in the NH stretch region (3300–3500 cm⁻¹) is shown in Figure 3b (top, black). This region is highly sensitive to the intramolecular hydrogen bonding architecture of the peptide and is commonly used to make unique structural assignments of peptides when supported by the sufficient theory. The NH stretch region shows three transitions, as anticipated given the three NH groups in the molecule. Two weak, narrow transitions are found in the free amide NH stretch region at 3466.2 and 3478.5 cm⁻¹. The intense, broad transition at 3361 cm⁻¹ indicates that the third NH bond is involved in a strong hydrogen bond. The calculated stick spectrum shown below the experimental spectrum belongs to the global minimum structure and is our best fit to the experimental spectrum. Its close match with the experiment across the NH stretch, amide I, and amide II regions lends confidence to the assignment.

The assigned structure has a single C10 hydrogen bond and is labeled as F-F-10 in our nomenclature, with ϕ_2/ψ_2 Ramachandran angles of $-59^\circ/115^\circ$ and ϕ_3/ψ_3 of $+58^\circ/+30^\circ$, matching those characteristics of a type II β -turn. The formation of a β -turn instead of a 3_{10} -helix is a straightforward result of the central amide group in the backbone being unconstrained by hydrogen bond formation because of the short length of the capped dipeptide. The loss of stabilization from an additional hydrogen bond on the central amide results in the unconstrained β -turn being the more stable structure.

3.3. Ac-(Aib)₂-NHBn-F. The R2PI spectrum in the S_0 - S_1 origin region for the NHBn-F-capped dipeptide is shown in Figure 4a. It was taken with a power 75% less than in NHBn to

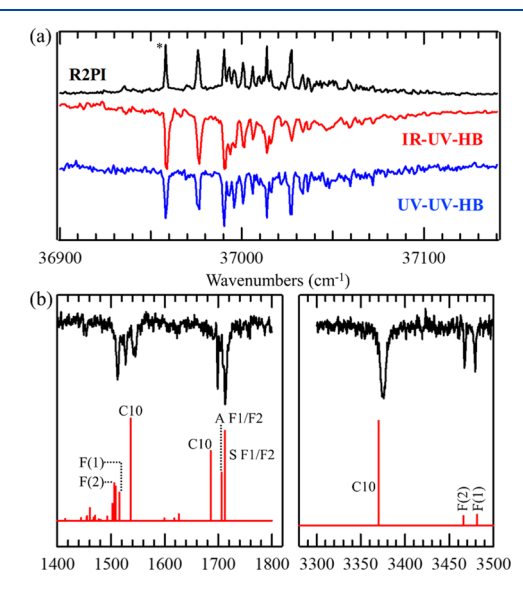


Figure 4. Single and double resonance spectra for Ac-Aib₂-NHBn-F. (a) R2PI spectrum (black, top), UV–UV HB (blue, bottom), and IR–UV HB scans (red, middle). The asterisk labels the peak used to monitor transition in obtaining the RIDIR spectrum. (b) RIDIR spectra in the amide I, amide II, and NH stretch regions, compared with the predictions of theory for the assigned structure. See the text for further discussion.

avoid saturation effects (not seen in NHBn), demonstrating the positive benefits of the larger UV oscillator strength of the NHBn-F cap. Importantly, the increased oscillator strength of the S_0 – S_1 transition allowed UV–UV HB spectra (bottom, blue) to be acquired, which is difficult with NHBn caps, and was one of the main motivations for considering this fluorinated phenyl cap. An IR–UV HB scan is also shown for comparison (middle, red). Being able to record UV–UV HB scans is significant because the UV spectra typically suffer

from less overlap than IR spectra, affording better specificity when selecting conformer-specific transitions for double resonance methods. Because all transitions in the R2PI spectrum are also present in the hole-burn scans, there is one major conformer in the expansion, despite the presence of more than 10 transitions in the UV region.

The RIDIR spectrum in Figure 4b is virtually identical to the corresponding spectrum acquired for NHBn (Figure 3b), indicating that the structures are very similar. Two free NH transitions are identified at 3467 and 3479 cm⁻¹ and a third, broad transition belonging to a C10 hydrogen bond is located at 3375 cm⁻¹. Indeed, the best fit structure is another type-II β -turn that has nearly identical ϕ/ψ angles (Table 1) to the

Table 1. List of Dihedrals, Hydrogen Bond Lengths, and Hydrogen Bond Angle for the NHBn β -Turn Structures, Obtained from DFT Calculations^a

	ϕ_1 (deg)	ψ_1 (deg)	$\phi_2 \ (ext{deg})$	ψ_2 (deg)	l _{Hbond} (Å)	∠COH (deg)
type II β -turn	-60	120	80	0		
NHBn	-59	115	58	30	1.96	120
NHBn-F	-59	116	59	30	1.96	120
AMBA Conf A	-60	117	58	30	1.96	121

^aDihedrals start from the N-terminus.

assigned structure of NHBn. We surmise on this basis that fluorine substitution on the phenyl ring does not perturb the structure significantly. Because the F-F-10 conformer, like its NHBn counterpart, does not contain an NH··· π interaction, it is not possible to evaluate the extent to which fluorine substitution on the aromatic ring reduces the strength of π ···H hydrogen bonds. A spectroscopic difference between the NHBn and NHBn-F caps becomes apparent in the 1400–1600 cm⁻¹ region, typically ascribed to amide II vibrations. However, in the spectrum of the NHBnF-capped molecule, a new transition appears at 1527.5 cm⁻¹, which is due to the C–F stretch fundamental. If the fluorine atom is involved in intramolecular or intermolecular bonding, it is possible that the C–F transition could have structural diagnostic capabilities in future studies.

3.4. Ac-(Aib)₂-AMBA. The R2PI spectrum of the AMBA-capped dipeptide in the S_0 – S_1 origin region is shown in Figure 5a (top, black). IR–UV HB scans are shown below the R2PI spectrum, demonstrating the presence of two conformers with S_0 – S_1 origin transitions at 37 562 cm⁻¹ (conformer A, blue) and 37 462 cm⁻¹ (conformer B, red). The small band +22 cm⁻¹ above the B origin does not appear in the IR–UV HB spectrum and thus must be due to a third minor conformer. Given the small size of this transition, we did not pursue its characterization further.

RIDIR spectra were collected while monitoring both origin peaks, with results shown in Figure 5b. Incorporation of the AMBA cap was intended to create two diastereomers out of otherwise indistinguishable R- and L-handed structural pairs. However, inspection of the NH stretch RIDIR spectra (Figure 5b) indicates that conformer A (blue, bottom) and conformer B (red, top) have different hydrogen bonding networks. Indeed, cursory inspection shows one (conformer B) and two (conformer A) free NH stretch fundamentals, eliminating them as members of a diastereomeric pair. Conformer A of AMBA shows the same hydrogen bonding pattern as the sole

The Journal of Physical Chemistry A

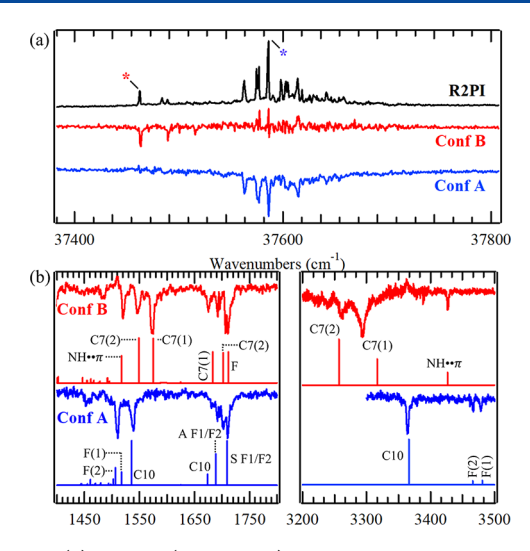


Figure 5. (a) R2PI (top, black) and IR–UV HB spectra for conformer A (bottom, blue) and conformer B (middle, red) of AMBA, respectively. The asterisk indicates the frequency of the UV laser to produce the RIDIR spectra (b), with the color matched to the respective conformer. (b) RIDIR spectra for conformers A and B of AMBA in the NH stretch region (3200–3500 cm⁻¹) and amide I/II regions (1400–1800 cm⁻¹). Stick spectra are the predictions of scaled, harmonic vibrational frequency calculations for the two assigned structures. F indicates transitions involving free N–H bonds, Cn indicates hydride stretches that close rings containing n atoms, A indicates antisymmetric transition, and S indicates symmetric transition.

conformers of NHBn, with two free NH transitions at 3467 and 3479 cm⁻¹ and a broad transition belonging to a C10 hydrogen bond at 3585 cm⁻¹. Not surprisingly, the structure is assigned to the same type II β -turn as in NHBn and NHBn-F. By contrast, conformer B of AMBA shows only one peak above 3400 cm⁻¹, assigned to an amide NH $\cdots\pi$ stretch at 3426.4 cm⁻¹. The experimental spectrum of conformer B shows two broadened transitions at 3293.5 and 3260.5 cm⁻¹, with the latter particularly broadened and split, complicating the matchup between experiment and theory. However, the excellent match in the amide I/II regions strengthens the assignment of conformer B to a structure with a sequential C7-C7 double ring, with two γ-turns of first left- and then right-handed orientation. This structure is similar to a β ribbon, and we refer to it as a 27-ribbon.8 It is also worth noting that C7 hydrogen bonds often exhibit broadened NH stretch fundamentals, as seen in previous work with Aib peptides.31

The assigned structures for all observed conformers of the three capped peptides are presented in Figure 6. Despite the different nature of the caps, the same β -turn structure is observed in all three molecules, with NHBn and NHBn-F having it as the only observed conformer. The striking similarity is also evident in the ϕ/ψ Ramachandran angles, hydrogen bond lengths, and NHO bond angles presented in Table 1. When the chiral AMBA cap is present, a second important conformer is present, the 2_7 -ribbon. The increase in the population of this conformer based on the addition of a methyl group to $C(\alpha)$ is slightly surprising, as adding a methyl group outside of the folding region of the peptide would not be expected to perturb the intramolecular interactions and the methyl group can only provide stabilization through weak dispersive interactions. We believe that preferential stabiliza-

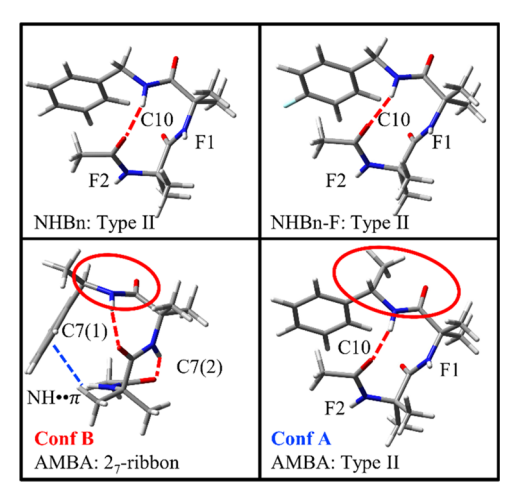


Figure 6. Comparison of the structures assigned for NHBn (top, left), NHBn-F (top, right), and AMBA (bottom).

tion of the 2_7 -ribbon by the methyl group seems less likely than a destabilizing effect of the methyl group because of steric effects in the β -turn structure, discussed in greater detail in Section 4.2.

4. DISCUSSION

4.1. Comparison of Z-Aib₂-OMe and Z-Aib₄-OMe. Previous work on Aib dipeptides³¹ utilized an N-terminal benzyloxycarbonyl (Z) cap to sensitize Aib₂-OMe for UV and IR-UV double resonance experiments. Gord et al. showed that Z-Aib₂-OMe adopts three different conformers, an F-5 conformer, an F-7/5 structure with a unique C7/C5 bifurcated hydrogen bond, and an extended 5-5 structure. The dihedral angles for these conformers are included in Table 2. An important distinction between the capping groups used by Gord et al. (N-terminal Z cap and C-terminal OMe cap) and the caps used in this study (Ac N-terminal and NHBn Cterminal cap) is how the caps alter the number of hydrogen bond donor/acceptor groups. Z-Aib₂-OMe has only two amide NH groups, whereas Ac-Aib2-R caps studied here all incorporate three. To that end, Z-Aib2-OMe cannot form a C10 hydrogen bond, precluding the formation of a β -turn. Nevertheless, conformers were identified, which are preconfigured for 3₁₀-helix formation, at least in part. This is particularly true of the F-5 structure, which was the global minimum energy conformer (Table 2).

In the capped Ac-Aib₂-R dipeptides studied here, the global minimum is a structure with a single C10 hydrogen bond. However, while the dihedral angles associated with the Aib(2) residue are those of a 3_{10} -helix, Aib(1) takes on dihedrals ($\phi_1 = -59^{\circ}$, $\psi_1 = +116^{\circ}$) that enable formation of a type II β -turn. We will return to this point when considering energetic grounds shortly. The steric influence of the α -dimethyl residue of Aib amino acids leads to the formation of a 3_{10} -helix in the gas phase once there are two or more C10 hydrogen bonds possible, which reorient the central amide group(s) to form these additional hydrogen bonds. We will provide a more in-depth exploration in Section 4.2 of what forces may contribute to the unexpected formation of the type II β -turn over the expected 3_{10} -helix.

The IR spectroscopy itself provides some evidence that the C10 hydrogen bond in the type II β -turn is slightly stronger than the type III C10 hydrogen bond of the 3_{10} -helix. Recall

The Journal of Physical Chemistry A

Table 2. List of Dihedrals, Hydrogen Bond Length, and Hydrogen Bond Angle for the NHBn β -Turn and 3_{10} -Helix-like Structures, Obtained from DFT Calculations^a

	assigned 2° structure	H-bonds	ϕ_1	ψ_1	ϕ_2	ψ_2	ϕ_3	ψ_4
type II/II' β -turn			∓60	±120	±80	<u>±</u> 0		
3 ₁₀ -helix (right)			-57	-30	-57	-30		
NHBn	type II	F-F-10	-59	115	58	30		
NHBn-F	type II	F-F-10	-59	116	59	30		
AMBA (A)	2 ₇ -ribbon	$\pi - 7 - 7$	-75	60	68	-71		
AMBA (B)	type II	F-F-10	-60	117	59	30		
AMBA-F (crystal)	type III	F-F-10	-55	-35	-62	-23		
AMBA (theory)	type II'	F-F-10	57	-122	-58	-34		
3 ₁₀ -helix-like		F-F-10	-67	-14	-53	-35		
Z -Aib ₂ -OMe $(A)^b$		F-5	-57	-38	-178	-179		
Z-Aib ₂ -OMe $(B)^b$		F-7/5	-72	70	180	179		
Z -Aib ₂ -OMe $(C)^b$		5-5	180	-180	180	180		
Z -Aib ₄ -OMe $(S)^b$	3 ₁₀ -helix	F-F-10-7	-61	-26	-55	-31	51	40
Z -Aib ₄ -OMe $(NS)^b$	3 ₁₀ -helix	F-F-10-7	-61	-27	-57	-22	-48	-40

^aDihedrals start from the N-terminus. F represents free and numerals *n* represent C*n* hydrogen bonds, starting with the N-terminus and progressing toward the C-terminus. ^bRef 31. S represents a Schellman motif, NS represents a non-Schellman motif.

that the vibrational transitions in the NH stretch region of NHBn, NHBn-F, and AMBA Conf B contain two free NH transitions at ~3466 and ~3479 cm⁻¹ and a strong, broad transition at ~3361 cm⁻¹. Z-Aib₄-OMe also has two free NH stretch fundamentals at 3467 and 3478 cm⁻¹ and two hydrogen-bonded NH stretches at 3383 and 3406 cm⁻¹. While the intensity patterns between the spectra of Z-Aib₄OMe and the Ac-Aib₂-R series are strikingly similar, the hydrogen-bonded NH stretch fundamental in the Ac-Aib₂-R peptides is shifted 20 cm⁻¹ lower in frequency than the lowest energy transition found in Z-Aib₄-OMe. This suggests the presence of a stronger C10 hydrogen bond in the Ac-Aib₂-R peptide β -turns than in the 3₁₀-helix of Z-Aib₄-OMe. The strength of this hydrogen bond likely contributes to the formation of the β -turn over the formation of the 3₁₀-helix, as is discussed further below.

4.2. Energetic Analysis. Figure 7a presents energy level diagrams for each member of our series, depicting the relative zero-point-corrected energies of all conformers within 20 kJ/ mol of the global minimum for each member of our series. The assigned structures for the NHBn and NHBn-F caps are both type II β -turns, while the chiral AMBA cap had population in both a type II β -turn and a 2₇-ribbon conformation. For NHBn and NHBn-F, the DFT calculations predict that the β -turn is the global minimum structure. The next lowest energy structure in both conformers, ~3 kJ/mol higher in energy, is a 2₇-ribbon nearly identical to the assigned structure for AMBA conformer B. Notably, in AMBA, the 27-ribbon structure drops in energy relative to the type II β -turn, becoming more stable than the type II β -turn by 0.5 kJ/mol. This stabilization is consistent with the experimental detection of the 27 ribbon in the presence of the AMBA cap. In the 27-ribbon structure of AMBA, the α -methyl group that renders the benzylic carbon chiral points away from the rest of the molecule and likely has little interaction, suggesting that its effect on the 27-turn energetics is small. It seems more likely, then, to ascribe the energy difference in AMBA relative to NHBn to the destabilizing steric effect of the methyl group on the type II β -turn, a change in relative energy of 3.4 kJ/mol.

A structure with Ramachandran angles similar to a 3₁₀-helix (in green, Figure 7a) was located in each of the capped Aib dipeptides, as might have been anticipated based on the 3₁₀-

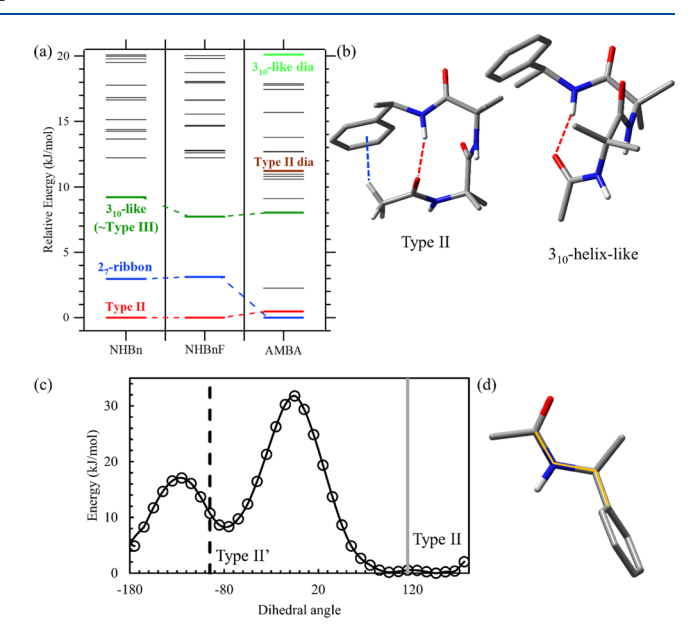


Figure 7. (a) Potential energy diagram for Ac-Aib₂-R, where the R label is given on the *x*-axis. Zero-point-corrected relative energies at the DFT B3LYP/6-31(g)+d level of theory with the D3BJ dispersion correction. (b) Comparison of β -turn (left) to 3₁₀-helix-like conformation (right), with nonpolar hydrogens removed to improve clarity. Red lines indicate hydrogen bonds, and blue lines indicate *π*-interactions. (c) Relative energy vs dihedral angle along the coordinate indicated in (d) by an orange line. The same level of theory was used as in (a). (d) Image to illustrate which dihedral coordinate was scanned.

helix folding propensity of oligo-Aib peptides. This structure is compared with the type II β -turn in Figure 7b. Note that the principle difference between the two is the orientation of the central amide group. In the 3_{10} -helix-like structure (hereafter referred to as 3_{10} -like), the central C=O group points in the same direction along the helix as those adjacent to it, as it must if it is to form a hydrogen bond in a longer 3_{10} -helix.

In all three capped dipeptides, the 3_{10} -helix-like conformer is 8-10 kJ/mol above the global minimum. Typical ϕ/ψ angles for a 3_{10} -helix with several complete turns are loosely defined because of strain from direct overlap between the i and i+3

residues of the peptides, preventing the formation of perfect (e.g., idealized) 3_{10} -helices. The ϕ/ψ angles are usually around $-57^\circ/-30^\circ$ for ϕ_1/ψ_1 and ϕ_2/ψ_2 . The $\phi+\psi$ sums typically range between -90° and -120° , which is close to the sum of the first set of ϕ/ψ angles of a type II β -turn, explaining the similarity of the structures. In the type II β -turn, the ϕ_2/ψ_2 angles are $-59^\circ/115^\circ$, whereas in the 3_{10} -helix-like structure, the ϕ/ψ angles are $-53^\circ/-35^\circ$. As discussed above, the type II β -turn may be more likely to form in the short peptides studied here because the unconstrained central amide group does not need to be involved in hydrogen bonding present in the 3_{10} -helix. It may also be inferred based on the results from Z-Aib $_4$ -OMe that the 3_{10} -helix forms a weaker C10 hydrogen bond than the β -turn, as discussed earlier 31

Depending on the barriers to conformational isomerization and the timescales for cooling, conformer populations can sometimes be dictated more by their equilibrium populations [via $\Delta G(T)$] prior to cooling rather than by their zero-point-corrected relative energies. To investigate the populations at these temperatures, we calculated ΔG (300 K) for all conformers of the NHBn- and AMBA-capped dipeptides with zero-point energies below 10 kJ/mol. The free energy diagram is shown in Figure S2, with an emphasis on ΔE in the diastereomer of the type II β -turn, which is potentially more stable according to ΔG values. Note that because laser desorption was used to bring the samples into the gas phase, we have no direct measure of the appropriate temperature to use; hence, the choice of $T_{\rm conformer}$ = 300 K is used to track how the conformer populations respond to increasing temperature.

The structure with the lowest free energy did not change in either molecule, nor did the ordering of all structures below 5 kJ/mol, indicating that our focus on zero-point-corrected internal energies is justified. At the same time, all conformers seem to have a relative free energy closer to that of the global minimum than was the case in the zero-point energy-corrected internal energies. In particular, the 3₁₀-like structures are lower in relative free energies by ~4 kJ/mol in NHBn and ~6 kJ/mol in AMBA compared to the type II β -turn. Furthermore, the diastereomer of the type II β -turn lowers from 11 kJ/mol in ΔE to 5 kJ/mol in ΔG . While none of these conformers had population trapped in them by the jet-cooling process, it is interesting to see that the free energies suggest that both the 3_{10} -helix and the type II' β -turn diastereomer are close enough in free energy to the type II β -turn that further modification of the position/nature of the cap or elongation of the Aib oligomer could bring them into competition.

Indeed, in considering how the caps might affect the energetics, we have also considered the $CH_3-\pi$ interaction present in the type II β -turn (Figure 7b). To investigate the influence of the aromatic ring cap computationally, we reoptimized all structures below 15 kJ/mol after substituting a methyl group for the phenyl ring so that NHBn becomes NHEt. The relative energies of the ethyl-capped structures can be found in Figure S1. The type II β -turn remains the global minimum energy structure with the NHEt cap, indicating that the primary forces driving the formation of the β -turn are not linked to the aromatic ring. The 2_7 -ribbon, which has an NH $-\pi$ interaction, increases its relative energy from 3.0 to 4.6 kJ/mol in the absence of the phenyl ring.

One of the most striking energetic changes between the NHBn and NHEt caps is that the 3₁₀-like helix collapses from 9.2 kJ/mol in relative energy to 1.1 kJ/mol, adopting a different structure that becomes the second lowest energy

conformer. The new structure has ψ_1/ϕ_1 angles of -61° and -28° and ψ_2/ϕ_2 angles of -62° and -20° , which fall within the range of the ϕ/ψ angles of the first turn of a 3_{10} -helix. Additionally, two other structures, found at 13.6 and 14.2 kJ/mol, which were phenyl rotors of the 3_{10} -like helix (Figure S1), were optimized to the same structure. These results suggest that the phenyl ring of the NHBn cap creates unfavorable interactions that hinder the formation of the 3_{10} -helix. Though this result is interesting, the type II β -turn remains the calculated global minimum in both the presence and absence of the phenyl ring cap.

A principal reason for considering the chiral AMBA cap is that it would enable us to distinguish right- and left-handed structures in the otherwise achiral Aib dipeptide. The energy level diagram in Figure 7a shows the presence of a significant energy difference between the left-handed and right-handed diastereomeric structures created by the S-chiral AMBA cap. Surprisingly, the left-handed diastereomer of the lowest energy right-handed β -turn conformer, which we label as type II', is found 11.2 kJ/mol above the global minimum, indicating that the steric differences between left- and right-handed β -turns are significant. To explain this difference, we consider the chiral center associated with the AMBA cap and how it interacts with the rest of the molecule. In the type II' diastereomeric structure, the methyl group of the AMBA cap is cis to the nearest acyl group, whereas it is trans in the type II structure, indicating the presence of an unfavorable steric interaction between the methyl and acyl groups (Figure 6). It is initially surprising that this interaction would result in an 11 kJ/mol difference in energy.

To investigate the energetic cost of eclipsing the acyl group with the methyl group of the AMBA cap, we performed a relaxed dihedral scan of an AMBA fragment, N-1-(phenylethyl)acetamide (shown in Figure 7d), along a dihedral between the acyl and methyl group (acyl/methyl dihedral), highlighted in orange on the model. All other initial dihedral angles match the lowest energy type II β -turn, shown in Figure 7b. The energy difference of the fragment when the dihedral angle matches the type II β -turn diastereomers is 10.2 kJ/mol, a value in reasonable agreement with the fully optimized structures. Although the dihedral scan of N-1(phenylethyl)acetamide does not provide a perfect account for the energetic cost of eclipsing the acyl and methyl group of the AMBA cap, it does point toward this interaction as the major determinant in destabilizing the left-handed type II' β -turn relative to the right-handed type II turn. A similar comparison between the diastereomers of the 3₁₀-like structures shows a similar difference in energy (~10 kJ/mol), also shown in Figure 7a, consistent with the energetic cost of the aforementioned cis acyl/methyl group.

4.3. Comparison of X-ray Data. As a further point of comparison with the gas-phase conformational results for Ac-Aib₂-AMBA, we obtained single-crystal X-ray diffraction results for its para-fluorinated analogue, Ac-Aib₂-AMBA-F. This molecule crystallized as a monohydrate with four peptide molecules per unit cell (Figure S3). Interestingly, the peptide crystallized in a right-handed β -turn, with a single C10 intramolecular hydrogen bond (see the Supporting Information for .cif file), as in the gas phase. However, peptide molecules in the crystalline solid exhibit a type III β -turn rather than the type II turn found as the global minimum in the gas phase. The preference for the right-handed type III turn over left-handed type III' must presumably be imposed by the S-

configuration of the C-terminal AMBA-F group, with the intramolecular methyl/acyl interaction likely contributing to the preference for the right-handed over left-handed β -turn.

The peptides and water molecules of the crystalline structure exhibit significant *intermolecular* hydrogen bonding, further stabilizing the observed type III configurations. The positions of hydrogen atoms suggest more than twice as many hydrogen bonding interactions between cocrystallized water and peptide molecules than C10-type intramolecular hydrogen bonds within the peptide molecules themselves. Therefore, we attribute the discrepancy between the crystal structure and our gas-phase structural determination to the significant structural influence of hydrogen bonding interactions with cocrystallized water and with neighboring molecules in the crystal lattice.

5. CONCLUSIONS

Three chromophore caps were tested on a model Aib dipeptide system. The addition of fluorine to the NHBn fluorophore produced no significant structural perturbation while affording increased signal and UV-UV HB capabilities. The addition of a chiral methyl group to the benzyl carbon in AMBA induces a strong, destabilizing steric interaction between the methyl substituent and the nearest amide carbonyl. Inspection of the energy level diagram for AMBA indicates that the oppositely handed β -turn is ~11 kJ/mol above the global minimum. Finally, because of the improved signal and hole-burning capabilities arising using the NHBn-F cap, we plan in future studies to carry out single-conformation spectroscopy on Ac-Aib₃-AMBA-F with the goal of determining whether the large energy gap calculated to exist in Ac-Aib₂-AMBA-F is mitigated by increasing the length of the peptide and therefore the number of C10 hydrogen bonds present. The search for a chiral cap that interacts less strongly with the adjacent amide group will also be pursued. The extension to a longer Aib oligomer is crucial because Aib, is too short to form a single turn of a helix, while Aib₃ can do so. This will provide the first opportunity to see and characterize both handed helices in the gas phase.

ASSOCIATED CONTENT

S Supporting Information

The Supporting Information is available free of charge on the ACS Publications website at DOI: 10.1021/acs.jpca.9b01698.

Image of crystal structures and experimental details used for acquiring crystallographic data (PDF)

Crystallographic data of AMBA-F (CIF)

AUTHOR INFORMATION

Corresponding Author

*E-mail: Zwier@purdue.edu (T.S.Z.).

ORCID

Joshua L. Fischer: 0000-0001-6183-8606 Karl N. Blodgett: 0000-0002-6827-0328 Matthias Zeller: 0000-0002-3305-852X Timothy S. Zwier: 0000-0002-4468-5748

Author Contributions

The manuscript was written through contributions of all authors. All authors have given approval to the final version of the manuscript.

Notes

The authors declare no competing financial interest.

ACKNOWLEDGMENTS

J.L.F., K.N.B., and T.S.Z. gratefully acknowledge support for this work from the National Science Foundation under grant NSF CHE-1764148. B.R.E. was supported by a Hardiman grant from the Provost's Office of Fairfield University. Funding for the single-crystal X-ray diffractometer was supported by the National Science Foundation through the Major Research Instrumentation Program under grant no. CHE 1625543.

REFERENCES

- (1) Dill, K. A. Dominant forces in protein folding. *Biochemistry* **1990**, 29, 7133–7155.
- (2) Dill, K. A.; Ozkan, S. B.; Shell, M. S.; Weikl, T. R. The protein folding problem. *Annu. Rev. Biophys.* **2008**, *37*, 289–316.
- (3) Nick Pace, C.; Scholtz, J. M.; Grimsley, G. R. Forces stabilizing proteins. FEBS Lett. 2014, 588, 2177–2184.
- (4) Eisenberg, D. The discovery of the -helix and -sheet, the principal structural features of proteins. *Proc. Natl. Acad. Sci. U.S.A.* **2003**, *100*, 11207–11210.
- (5) Donohue, J. Hydrogen bonded helical configurations of the polypeptide chain. *Proc. Natl. Acad. Sci. U.S.A.* **1953**, *39*, 470–478.
- (6) Venkatachalam, C. M. Stereochemical criteria for polypeptides and proteins. V. Conformation of a system of three linked peptide units. *Biopolymers* **1968**, *6*, 1425–1436.
- (7) O'Neil, K.; DeGrado, W. A thermodynamic scale for the helix-forming tendencies of the commonly occurring amino acids. *Science* **1990**, 250, 646–651.
- (8) Pauling, L.; Corey, R. B.; Branson, H. R. The structure of proteins: two hydrogen-bonded helical configurations of the polypeptide chain. *Proc. Natl. Acad. Sci. U.S.A.* 1951, 37, 205–211.
- (9) Anderson, C. A. F.; Rost, B. Structural Bioinformatics. In *Structural Bioinformatics*, 2nd ed.; Gu, J., Weissig, H., Eds.; John Wiley & Sons, Inc.: Hoboken, 2003; pp 339–363.
- (10) Toniolo, C.; Benedetti, E. The polypeptide 310-helix. *Trends Biochem. Sci.* **1991**, *16*, 350–353.
- (11) Beck, D. A. C.; Alonso, D. O. V.; Inoyama, D.; Daggett, V. The intrinsic conformational propensities of the 20 naturally occurring amino acids and reflection of these propensities in proteins. *Proc. Natl. Acad. Sci. U.S.A.* **2008**, *105*, 12259–12264.
- (12) Atilgan, C.; Gerek, Z. N.; Ozkan, S. B.; Atilgan, A. R. Manipulation of Conformational Change in Proteins by Single-Residue Perturbations. *Biophys. J.* **2010**, *99*, 933–943.
- (13) Park, S. H.; Opella, S. J. Conformational changes induced by a single amino acid substitution in the trans-membrane domain of Vpu: Implications for HIV-1 susceptibility to channel blocking drugs. *Protein Sci.* **2007**, *16*, 2205–2215.
- (14) Toniolo, C.; Bonora, G. M.; Barone, V.; Bavoso, A.; Benedetti, E.; Di Blasio, B.; Grimaldi, P.; Lelj, F.; Pavone, V.; Pedone, C. Conformation of pleionomers of .alpha.-aminoisobutyric acid. *Macromolecules* 1985, 18, 895–902.
- (15) Marshall, G. R.; Hodgkin, E. E.; Langs, D. A.; Smith, G. D.; Zabrocki, J.; Leplawy, M. T. Factors governing helical preference of peptides containing multiple alpha,alpha-dialkyl amino acids. *Proc. Natl. Acad. Sci. U.S.A.* **1990**, 87, 487–491.
- (16) Bavoso, A.; Benedetti, E.; Di Blasio, B.; Pavone, V.; Pedone, C.; Toniolo, C.; Bonora, G. M. Long polypeptide 310-helices at atomic resolution. *Proc. Natl. Acad. Sci. U.S.A.* 1986, 83, 1988–1992.
- (17) Jones, J. E.; Diemer, V.; Adam, C.; Raftery, J.; Ruscoe, R. E.; Sengel, J. T.; Wallace, M. I.; Bader, A.; Cockroft, S. L.; Clayden, J.; Webb, S. J. Length-Dependent Formation of Transmembrane Pores by 310-Helical α -Aminoisobutyric Acid Foldamers. *J. Am. Chem. Soc.* **2016**, *138*, 688–695.
- (18) Maekawa, H.; Formaggio, F.; Toniolo, C.; Ge, N.-H. Onset of 310-Helical Secondary Structure in Aib Oligopeptides Probed by

- Coherent 2D IR Spectroscopy. J. Am. Chem. Soc. 2008, 130, 6556-6566.
- (19) Zeko, T.; Hannigan, S. F.; Jacisin, T.; Guberman-Pfeffer, M. J.; Falcone, E. R.; Guildford, M. J.; Szabo, C.; Cole, K. E.; Placido, J.; Daly, E.; Kubasik, M. A. FT-IR Spectroscopy and Density Functional Theory Calculations of 13C Isotopologues of the Helical Peptide Z-Aib6-OtBu. *J. Phys. Chem. B* **2014**, *118*, 58–68.
- (20) Cable, J. R.; Tubergen, M. J.; Levy, D. H. Electronic spectroscopy of small tryptophan peptides in supersonic molecular beams. J. Am. Chem. Soc. 1988, 110, 7349–7355.
- (21) Cable, J. R.; Tubergen, M. J.; Levy, D. H. Fluorescence spectroscopy of jet-cooled tryptophan peptides. *J. Am. Chem. Soc.* 1989, 111, 9032–9039.
- (22) Rijs, A. M.; Oomens, J. Gas-Phase IR Spectroscopy and Structure of Biological Molecules; Springer, 2015; Vol. 364.
- (23) Alauddin, M.; Biswal, H. S.; Gloaguen, E.; Mons, M. Intraresidue interactions in proteins: interplay between serine or cysteine side chains and backbone conformations, revealed by laser spectroscopy of isolated model peptides. *Phys. Chem. Chem. Phys.* **2015**, *17*, 2169.
- (24) Chin, W.; Piuzzi, F.; Dognon, J.-P.; Dimicoli, I.; Tardivel, B.; Mons, M. Gas Phase Formation of a 310-Helix in a Three-Residue Peptide Chain: Role of Side Chain-Backbone Interactions as Evidenced by IR–UV Double Resonance Experiments. *J. Am. Chem. Soc.* **2005**, *127*, 11900–11901.
- (25) Dian, B. C.; Longarte, A.; Zwier, T. S. Conformational dynamics in a dipeptide after single-mode vibrational excitation. *Science* **2002**, *296*, *2369*–*2373*.
- (26) Dian, B. C.; Longarte, A.; Winter, P. R.; Zwier, T. S. The dynamics of conformational isomerization in flexible biomolecules. I. Hole-filling spectroscopy of N-acetyl tryptophan methyl amide and N-acetyl tryptophan amide. *J. Chem. Phys.* **2004**, *120*, 133–147.
- (27) James, W. H.; Baquero, E. E.; Choi, S. H.; Gellman, S. H.; Zwier, T. S. Laser Spectroscopy of Conformationally Constrained α/β -Peptides: Ac-ACPC-Phe-NHMe and Ac-Phe-ACPC-NHMe. *J. Phys. Chem. A* **2010**, *114*, 1581–1591.
- (28) Dean, J. C.; Buchanan, E. G.; Zwier, T. S. Mixed 14/16 Helices in the Gas Phase: Conformation-Specific Spectroscopy of Z-(Gly)n, n = 1, 3, 5. *J. Am. Chem. Soc.* **2012**, *134*, 17186–17201.
- (29) Kusaka, R.; Zhang, D.; Walsh, P. S.; Gord, J. R.; Fisher, B. F.; Gellman, S. H.; Zwier, T. S. Role of Ring-Constrained γ -Amino Acid Residues in α/γ -Peptide Folding: Single-Conformation UV and IR Spectroscopy. *J. Phys. Chem. A* **2013**, *117*, 10847–10862.
- (30) Gord, J. R.; Walsh, P. S.; Fisher, B. F.; Gellman, S. H.; Zwier, T. S. Mimicking the First Turn of an α -Helix with an Unnatural Backbone: Conformation-Specific IR and UV Spectroscopy of Cyclically Constrained β/γ -Peptides. J. Phys. Chem. B **2014**, 118, 8246–8256.
- (31) Gord, J. R.; Hewett, D. M.; Hernandez-Castillo, A. O.; Blodgett, K. N.; Rotondaro, M. C.; Varuolo, A.; Kubasik, M. A.; Zwier, T. S. Conformation-specific spectroscopy of capped, gas-phase Aib oligomers: tests of the Aib residue as a 310-helix former. *Phys. Chem. Chem. Phys.* **2016**, *18*, 25512–25527.
- (32) Walsh, P. S.; Dean, J. C.; McBurney, C.; Kang, H.; Gellman, S. H.; Zwier, T. S. Conformation-specific spectroscopy of capped glutamine-containing peptides: role of a single glutamine residue on peptide backbone preferences. *Phys. Chem. Chem. Phys.* **2016**, *18*, 11306–11322.
- (33) Blodgett, K. N.; Zhu, X.; Walsh, P. S.; Sun, D.; Lee, J.; Choi, S. H.; Zwier, T. S. Conformer-Specific and Diastereomer-Specific Spectroscopy of $\alpha\beta\alpha$ Synthetic Foldamers: Ac-Ala- β ACHC-Ala-NHBn. *J. Phys. Chem. A* **2018**, *122*, 3697–3710.
- (34) Fricke, H.; Funk, A.; Schrader, T.; Gerhards, M. Investigation of Secondary Structure Elements by IR/UV Double Resonance Spectroscopy: Analysis of an Isolated β -Sheet Model System. *J. Am. Chem. Soc.* **2008**, *130*, 4692–4698.
- (35) Lee, J. J.; Albrecht, M.; Rice, C. A.; Suhm, M. A.; Stamm, A.; Zimmer, M.; Gerhards, M. Adaptive aggregation of peptide model systems. *J. Phys. Chem. A* **2013**, *117*, 7050–7063.

- (36) Schwing, K.; Reyheller, C.; Schaly, A.; Kubik, S.; Gerhards, M. Structural analysis of an isolated cyclic tetrapeptide and its monohydrate by combined IR/UV spectroscopy. *ChemPhysChem* **2011**, *12*, 1981–1988.
- (37) Řeha, D.; Valdes, H.; Vondrášek, J.; Hobza, P.; Abu-Riziq, A.; Crews, B.; de Vries, M. S. Structure and IR Spectrum of Phenylalanyl—Glycyl—Glycine Tripetide in the Gas-Phase: IR/UV Experiments, Ab Initio Quantum Chemical Calculations, and Molecular Dynamic Simulations. *Chem.—Eur. J.* **2005**, *11*, 6803—6817.
- (38) Rijs, A. M.; Kabeláč, M.; Abo-Riziq, A.; Hobza, P.; de Vries, M. S. Isolated gramicidin peptides probed by IR spectroscopy. *ChemPhysChem* **2011**, *12*, 1816–1821.
- (39) Barry, C. S.; Cocinero, E. J.; Çarçabal, P.; Gamblin, D. P.; Stanca-Kaposta, E. C.; Remmert, S. M.; Fernández-Alonso, M. C.; Rudić, S.; Simons, J. P.; Davis, B. G. "Naked" and Hydrated Conformers of the Conserved Core Pentasaccharide of N-linked Glycoproteins and Its Building Blocks. *J. Am. Chem. Soc.* **2013**, *135*, 16895–16903.
- (40) Stanca-Kaposta, E. C.; Çarçabal, P.; Cocinero, E. J.; Hurtado, P.; Simons, J. P. Carbohydrate-Aromatic Interactions: Vibrational Spectroscopy and Structural Assignment of Isolated Monosaccharide Complexes with p-Hydroxy Toluene and N-Acetyl l-Tyrosine Methylamide. *J. Phys. Chem. B* **2013**, *117*, 8135–8142.
- (41) Levene, P. A.; Steiger, R. E. The action of acetic anhydride on tertiary amino acids and dipeptides. On catalytic effects. The hydrolysis of acetyldipeptides. *J. Biol. Chem.* **1931**, 93, 581–604.
- (42) Paterson, Y.; Stimson, E. R.; Evans, D. J.; Leach, S. J.; Scheraga, H. A. Solution conformations of oligomers of α -aminoisobutyric acid. *Int. J. Pept. Protein Res.* **1982**, *20*, 468–480.
- (43) Weiner, P. K.; Kollman, P. A. AMBER: Assisted model building with energy refinement. A general program for modeling molecules and their interactions. *J. Comput. Chem.* **1981**, *2*, 287–303.
- (44) Frisch, M. J.; Trucks, G. W.; Schlegel, H. B.; Scuseria, G. E.; Robb, M. A.; Cheeseman, J. R.; Scalmani, G.; Barone, V.; Mennucci, B.; Petersson, G. A.; et al. *Gaussian 16, Revision B.01*; Gaussian, Inc.: Wallingford, CT, 2016.
- (45) Walsh, P. S.; Dean, J. C.; McBurney, C.; Kang, H.; Gellman, S. H.; Zwier, T. S. Conformation-specific spectroscopy of capped Glutamine-containing peptides: Role of a single glutamine residue on peptide backbone preferences. *Phys. Chem. Chem. Phys.* **2016**, *18*, 11306–11322.
- (46) Bruker, Apex3 v2017.3-0, SAINT V8.38A, Bruker AXS Inc.: Madison, WI, USA, 2016.
- (47) Sheldrick, G. M. A short history of SHELX. Acta Crystallogr., Sect. A: Found. Crystallogr. 2008, 64, 112–122.
- (48) Sheldrick, G. M. SHELXT— Integrated space-group and crystal-structure determination. *Acta Crystallogr., Sect. A: Found. Adv.* **2015**, *71*, 3–8.
- (49) Hübschle, C. B.; Sheldrick, G. M.; Dittrich, B. ShelXle: a Qt graphical user interface for SHELXL. J. Appl. Crystallogr. 2011, 44, 1281–1284.